

# Dislocations in cubic crystals described by discrete models

L.L. Bonilla<sup>a</sup>, A. Carpio<sup>b</sup>, I. Plans<sup>a</sup>,

<sup>a</sup>Modelización, Simulación Numérica y Matemática Industrial, Universidad Carlos III de Madrid, Avenida de la Universidad 30, 28911 Leganes, Spain

<sup>b</sup>Departamento de Matemática Aplicada, Universidad Complutense de Madrid, 28040 Madrid, Spain

---

## Abstract

Discrete models of dislocations in cubic crystal lattices having one or two atoms per unit cell are proposed. These models have the standard linear anisotropic elasticity as their continuum limit and their main ingredients are the elastic stiffness constants of the material and a dimensionless periodic function that restores the translation invariance of the crystal and induces the dislocation size. For these models, conservative and damped equations of motion are proposed. In the latter case, the entropy production and thermodynamic forces are calculated and fluctuation terms obeying the fluctuation-dissipation theorem are added. Numerical simulations illustrate static perfect screw and 60° dislocations for GaAs and Si.

**Key words:** Discrete elasticity, cubic crystals, dislocations, fluctuating hydrodynamics

**PACS:** 61.72.Bb, 05.45.-a, 82.40.Bj, 45.05.+x

---

## 1 Introduction

Heteroepitaxial growth is fundamental for manufacturing important nanoelectronic devices based on self-assembled quantum dots [1,2] or superlattices [3]. Powerful imaging techniques based on scanning probe microscopes have been developed which allow to monitor these crystal growth processes down to atomic distances. Moreover, these techniques help visualizing defects such as

---

Corresponding author.

Email addresses: bonilla@ing.uc3m.es (L.L. Bonilla),  
ana\_carpio@mat.ucm.es (A. Carpio), ignacio.plans@uc3m.es (I. Plans).

m is t dislocations [4,5,6,7] (which may act as nucleation sites for quantum dots [1]) down to their cores. Understanding epitaxial growth requires understanding and relating processes which cover a wide range of scales [8]. Other multiscale problems need to be solved if we try to understand how dislocations [9,10], grain boundaries [4], cracks [11] and other defects control the mechanical, optical and electronic properties of the resulting materials [12]. Understanding these multiscale processes requires understanding better the relation between the defects themselves and observed macroscopic behavior, which remains an active area of research. While over mesoscopic length scales a coarse grained description based on defect densities makes sense [13,14], the cores of defects need to be resolved on nanometric scales and then coupled to the coarser description. Coarse grained descriptions of dislocation dynamics include irreversible thermodynamics, as in the works by Holt [13] and by Rickman and Vinals [14], Boltzmann-type kinetic equations, as in the formulations by Groma and coworkers [15] (and references therein), or stochastic models [16]. The atomic scale near defects can be resolved by ab initio or molecular dynamics simulations, which are very costly at the present time. Thus, it is interesting to have systematic models of defect motion in crystals that can be solved cheaply, are compatible with elasticity and yield useful information about the defect cores and their mobility.

In a previous paper, we have proposed a discrete model of dislocations and their motion in cubic crystals with a one atom basis [17]. In this paper, we present an extension of our previous theory to treat crystals with two-atom basis in their primitive cells (such as the diamond and zinc-blende structures of silicon and gallium arsenide, respectively). Moreover, we explain how to include dissipation in the dynamics of the model and how to consider the effect of fluctuations by using the ideas of fluctuating hydrodynamics [18,19,20]. Our model covers length scales in the nanometer range. In principle, to make contact with existing mesoscopic theories [14,15,16], one should define a dislocation density tensor and coarse grain over length scales up to hundreds of nanometers. This is outside the scope of the present work.

The main ingredients entering our discrete model are the elastic stiffness constants of the material and a dimensionless periodic function that restores the translation invariance of the crystal and induces the dislocation size. To be precise, consider a simple cubic symmetry with one atom per lattice point. Firstly, we discretize space along the primitive vectors defining the unit cell of the crystal  $\mathbf{x} = (l; m; n)a$ , in which  $a$  is the length of the primitive cubic cell, and  $l, m$  and  $n$  are integer numbers. Secondly, we replace the gradient of the displacement vector  $\mathbf{u}_i(\mathbf{x}; y; z; t) = a u_i(l; m; n; t)$  ( $u_i(l; m; n; t)$  is a nondimensional vector) in the strain energy density by an appropriate periodic function of the discrete gradient,  $g(\mathbf{D}_j^+ u_i)$ : We shall define the discrete distortion tensor as

$$w_i^{(j)} = g(D_j^+ u_i); \quad (1)$$

$$D_1 u_i(l;m;n;t) = [u_i(l-1;m;n;t) - u_i(l;m;n;t)]; \quad (2)$$

etc., where  $g(x)$  is a periodic function of period one satisfying  $g(x) = x$  as  $x \rightarrow 0$ . The strain energy density for the discrete model is obtained by substituting the strain tensor in the usual strain energy density:

$$W = \frac{1}{2} c_{ijkl} e_{ij} e_{kl}; \quad (3)$$

$$c_{ijkl} = C_{12} \delta_{ij} \delta_{kl} + \frac{C_{11} - C_{12}}{2} (\delta_{ik} \delta_{jl} + \delta_{il} \delta_{jk}) + H \frac{\delta_{ik} \delta_{jl} + \delta_{il} \delta_{jk}}{2} \delta_{1i} \delta_{1j} \delta_{1k} \delta_{1l} + 2\delta_{2i} \delta_{2j} \delta_{2k} \delta_{2l} + 3\delta_{3i} \delta_{3j} \delta_{3k} \delta_{3l}; \quad (4)$$

$$H = 2C_{44} + C_{12} - C_{11}; \quad (5)$$

$$e_{ij} = \frac{1}{2} (w_i^{(j)} + w_j^{(i)}) = \frac{g(D_j^+ u_i) + g(D_i^+ u_j)}{2} \quad (6)$$

(sum over repeated indices is assumed). Here  $C_{12}$ ,  $C_{11} - C_{12} = 2$  are the usual Lamé coefficients if  $H = 0$  and therefore the crystal is isotropic. Summing over all lattice sites, we obtain the potential energy of the crystal:

$$V(u_i; g) = a^3 \sum_{l,m,n} W(l;m;n;t); \quad (7)$$

in which we have considered the strain energy density to be a function of the point  $W(u) = W(l;m;n;t)$ ,  $(l;m;n) = (x;y;z) = a$ . Next, we find the equations of motion with or without dissipation by the usual methods of classical mechanics. For conservative dynamics:

$$a^4 u_i(l;m;n;t) = \frac{1}{a} \frac{\partial V(u_k; g)}{\partial u_i(l;m;n;t)}; \quad (8)$$

or, equivalently (see Section 2) [17],

$$a^2 u_i = \sum_{j;k;l} D_j [c_{ijkl} g^0(D_j^+ u_i) g(D_l^+ u_k)]; \quad (9)$$

Here  $u_i = \partial^2 u_i / \partial t^2$  and the displacement vector is dimensionless, so that both sides of Eq. (9) have units of force per unit area. Let us now restore dimensional units to Equation (9), so that  $u_i(x;y;z) = a u_i(x=a;y=a;z=a)$ , then let  $a \rightarrow 0$ , use Eq. (9) and that  $g(x) = x$  as  $x \rightarrow 0$ . Then we obtain the usual Cauchy equations of linear elasticity:

$$\frac{\partial^2 \alpha_i}{\partial t^2} = \sum_{j,k,l} \frac{\partial}{\partial x_j} C_{ijkl} \frac{\partial \alpha_k}{\partial x_l} ; \quad (10)$$

provided the components of the distortion tensor are very small. Far from the core of a defect, the discrete gradient approaches the continuous one. Then, provided the slope  $g^0(0)$  is one in the appropriate units, the spatially discrete equations of motion become those of the anisotropic elasticity.

The periodic function  $g(x)$  ensures that sliding a plane of atoms an integer number of times the lattice distance  $a$  parallel to a primitive direction does not change the potential energy of the crystal. We choose

$$g(x) = \begin{cases} x; & -\frac{1}{2} \leq x < \frac{1}{2} \\ \frac{(1/2 - x)(1/2 + x)}{4}; & -\frac{1}{2} < x < \frac{1}{2} + 1 \end{cases} ; \quad (11)$$

which is periodically extended outside the interval  $(-1/2; +1/2)$  for a given  $2 \leq (0; 1/2)$ . To select  $\gamma$ , we calculate the Peierls stress needed to move a given dislocation as a function of  $\gamma$  and fit it to data from experiments or molecular dynamics calculations. Once the discrete model is specified, different dislocation configurations can be selected by requiring that their far field should adopt the well-known form of continuous elasticity [17].

The rest of the paper is organized as follows. In Section 2, we review the derivation of the governing equations with conservative dynamics for simple cubic symmetry, and give the numerical constructions of screw and edge dislocations. We use the well known screw and edge dislocations for anisotropic elasticity to set up the boundary conditions far from the dislocation core and the initial conditions in overdamped equations of motion. Numerical solution of these equations yields the static dislocation configuration of our discrete elasticity model. In Section 3 we include dissipation and fluctuations in the equations of motion. Dissipation is described by a Rayleigh dissipative function that is a quadratic functional of the strain rate tensor, which, in turn, depends on the discrete distortion tensor. Since the distortion tensor (containing finite differences of the displacement vector) and its rate are larger near the core of defects, we expect that dissipation will be stronger near the core of a moving dislocation than at its far field. Fluctuations are introduced via the fluctuation-dissipation theorem and they should be stronger near the core of moving dislocations. An extension of our ideas to crystals with more complicated symmetries requires formulating our equations in non-orthogonal coordinates, which is explained in Section 4. The equations of motion for two-atom bases are obtained in Section 5 and the corresponding screw and 60 perfect dislocations are calculated for diamond and zinc-blende structures. Section 6 contains our conclusions.

## 2 Conservative equations of motion for a simple cubic lattice

In this Section, we shall derive the equations of motion (9) for the conservative dynamics given by (8). Firstly, let us notice that

$$\begin{aligned} \frac{\partial W}{\partial u_i(l;m;n;t)} &= \frac{\partial W}{\partial e_{jk}} \frac{\partial e_{jk}}{\partial u_i(l;m;n;t)} = \frac{1}{2} \sum_{jk} \frac{\partial [g(D_j^+ u_k) + g(D_k^+ u_j)]}{\partial u_i(l;m;n;t)} \\ &= \frac{1}{2} \sum_{jk} g^0(D_j^+ u_k) \frac{\partial (D_j^+ u_k)}{\partial u_i(l;m;n;t)} + g^0(D_k^+ u_j) \frac{\partial (D_k^+ u_j)}{\partial u_i(l;m;n;t)}; \end{aligned} \quad (12)$$

where  $W$  is a function of the point  $(l^0; m^0; n^0)$ , and we have used the definition of stress tensor:

$$e_{ij} = \frac{\partial W}{\partial e_{ij}}; \quad (13)$$

and its symmetry,  $e_{ij} = e_{ji}$ . Now, we have

$$\frac{\partial}{\partial u_i(l;m;n;t)} [D_l^+ u_k(l^0; m^0; n^0; t)] = e_{ik} (e_{ll^0+1} - e_{ll^0}) \delta_{mm^0} \delta_{nn^0}; \quad (14)$$

and similar expressions for  $j = 2, 3$ . By using (12) – (14), we obtain

$$\frac{\partial}{\partial u_i(l;m;n;t)} \sum_{l^0; m^0; n^0} W(l^0; m^0; n^0; t) = \sum_j D_j [e_{ij} g^0(D_j^+ u_i)]; \quad (15)$$

In this expression, no sum is intended over the subscript  $i$ , so that we have abandoned the Einstein convention and explicitly included a sum over  $j$ . Therefore Eq. (8) for conservative dynamics becomes

$$a^2 u_i = \sum_j D_j [e_{ij} g^0(D_j^+ u_i)]; \quad (16)$$

which yields Eq. (9). Except for the factor  $g^0(D_j^+ u_i)$ , these equations are discretized versions of the usual ones in elasticity [21].

### 2.1 Static dislocations of the discrete model

To find the dislocation solutions of our model, we need the stationary solution of the anisotropic elasticity equations at zero applied stress corresponding to

the same type of dislocation. In all cases, the procedure to obtain numerically the dislocation from the discrete model is the same. We first solve the stationary equations of elasticity with appropriate singular source terms to obtain the dimensional displacement vector  $\mathbf{u}(\mathbf{x};\mathbf{y};z) = (u_1(\mathbf{x};\mathbf{y};z); u_2(\mathbf{x};\mathbf{y};z); u_3(\mathbf{x};\mathbf{y};z))$  of the static dislocation under zero applied stress. This displacement vector yields the far field of the corresponding dislocation for the discrete model, which is the nondimensional displacement vector:

$$U(l;m;n) = \frac{\mathbf{u}((l+i_1)a; (m+i_2)a; (n+i_3)a)}{a} : \quad (17)$$

Here  $0 < i_i < 1, i = 1;2;3$ , are chosen so that the singularity at  $x = y = z = 0$  does not coincide with a lattice point. For a sc crystal, it is often convenient to select the center of a unit cell,  $i_i = 1/2$ . We use the nondimensional static displacement vector  $U(l;m;n)$  defined by (17) in the boundary and initial conditions for the discrete equations of motion.

Take for example, a pure screw dislocation along the  $z$  axis with Burgers vector  $\mathbf{b} = (0;0;b)$  has a displacement vector  $\mathbf{u} = (0;0;u_3(\mathbf{x};\mathbf{y}))$  with  $u_3(\mathbf{x};\mathbf{y}) = b(2)^{-1} \tan^{-1}(y/x)$  [9]. The discrete equation for the  $z$  component of the nondimensional displacement  $u_3(l;m;t)$  is:

$$a^2 u_3 = C_{44} f D_1 [g(D_1^+ u_3) g^0(D_1^+ u_3)] + D_2 [g(D_2^+ u_3) g^0(D_2^+ u_3)] g : \quad (18)$$

Numerical solutions of Eq. (18) show that a static screw dislocation moves if an applied shear stress surpasses the static Peierls stress,  $\mathcal{F}^j < F_{cs}$ , but that a moving dislocation continues doing so until the applied shear stress falls below a lower threshold  $F_{cd}$  (dynamic Peierls stress); see Ref. [22] for a similar situation for edge dislocations. To find the static solution of this equation corresponding to a screw dislocation, we could minimize an energy functional. However, it is more efficient to solve the following overdamped equation:

$$u_3 = C_{44} f D_1 [g(D_1^+ u_3) g^0(D_1^+ u_3)] + D_2 [g(D_2^+ u_3) g^0(D_2^+ u_3)] g : \quad (19)$$

The stationary solutions of Eqs. (18) and (19) are the same, but the solutions of (19) relax rapidly to the stationary solutions if we choose appropriately the damping coefficient. We solve Eq. (19) with initial condition  $u_3(l;m;0) = U_3(l;m) - b(2a)^{-1} \tan^{-1}[(m+1/2)/(l+1/2)]$  (corresponding to  $i_i = 1/2$ ), and with boundary conditions  $u_3(l;m;t) = U_3(l;m) + Fm$  at the upper and lower boundaries of our lattice. At the lateral boundaries, we use zero-flux Neumann boundary conditions. Here  $F$  is an applied dimensionless stress with  $\mathcal{F}^j < F_{cs}$  (the dimensional stress is  $C_{44}F$ ). For this small stress, the solution of Eq. (19) relaxes to a static screw dislocation  $u_3(l;m)$  with the desired far field. Figure 3 of Ref. [17] shows the helical structure adopted by the deformed

lattice  $(l; m; n + u_3(l; m))$  for an asymmetric piecewise linear  $g(\mathbf{x})$  as in Eq. (10). The numerical solution shows that moving a dislocation requires that we should have  $g^0(D_j^+ u_3) < 0$  (with either  $j = 1$  or  $2$ ) at its core [22], which is harder to achieve as  $\epsilon$  decreases. A discussion of the changes in the size of the dislocation core and the Peierls stress due to  $\epsilon$  can be found in Ref. [17]; see in particular Figure 2. Using the same technique, stationary planar edge dislocations for an isotropic sc material have been constructed and a variety of dipole and loops of edge dislocations have been numerically found [17].

### 3 Dissipative equations of motion and fluctuations

#### 3.1 Equations of motion including dissipation

Overdamped dynamics obtained by replacing the time differential of the displacement vector instead of the inertial term in the equation of motion (9) is not too realistic. Instead, we can add dissipation to the equations of motion by considering a quadratic dissipative function with cubic symmetry:

$$R = \frac{2}{3} \frac{\epsilon_{11}^2}{2} + \epsilon_{ik}^2 + \frac{1}{2} (\epsilon_{ik} - \epsilon_{11} \delta_{i1} \delta_{k1} - \epsilon_{22} \delta_{i2} \delta_{k2} - \epsilon_{33} \delta_{i3} \delta_{k3})^2 \quad (20)$$

For an isotropic body, we have  $\epsilon = 0$  and then  $\eta$  and  $\zeta$  are the usual viscosities; see Eq. (34.5) in Ref. [21]. The viscous part of the stress tensor is the symmetric tensor

$$\sigma_{ik} = \frac{\partial R}{\partial \epsilon_{ik}} = \eta_{iklm} \epsilon_{lm}; \quad (21)$$

$$\eta_{iklm} = \frac{1}{2} \left( \frac{2}{3} \delta_{ik} \delta_{lm} + \frac{1}{2} (\delta_{il} \delta_{km} + \delta_{im} \delta_{kl}) \right) + \frac{1}{2} \left( \frac{\delta_{il} \delta_{km} + \delta_{im} \delta_{kl}}{2} \delta_{1i} \delta_{1k} \delta_{1l} \delta_{1m} + \delta_{2i} \delta_{2k} \delta_{2l} \delta_{2m} + \delta_{3i} \delta_{3k} \delta_{3l} \delta_{3m} \right); \quad (22)$$

In the cubic case, the viscosity tensor  $\eta_{iklm}$  is determined by the three scalar quantities  $\eta$ ,  $\zeta$  and  $\epsilon$ . For isotropic sc crystals,  $\epsilon = 0$ . Similarly to Eq. (15), we can show that

$$\frac{\partial}{\partial u_i(l; m; n; t)} \sum_{l^0; m^0; n^0} R(l^0; m^0; n^0; t) = \sum_j^X D_j [ - \epsilon_{ij} g^0(D_j^+ u_i) ]; \quad (23)$$

is minus the dissipative force acting on  $u_i$ . Then the equation of motion including dissipation becomes

$$a^2 u_i = \sum_j D_j [(i_j + i_j) g^0 (\partial_j^+ u_i)] : (24)$$

In the isotropic case and taking the continuum limit  $a \rightarrow 0$ , Eqs. (24) with (21) and (22) yield the viscous Navier's equations for isotropic elasticity [21]:

$$\frac{\partial^2 \mathbf{u}}{\partial t^2} = -\mathbf{u} + (\lambda + \mu) \nabla (\nabla \cdot \mathbf{u}) + \frac{\partial \mathbf{u}}{\partial t} + \frac{\lambda}{3} \nabla \cdot \nabla \mathbf{u} : (25)$$

### 3.2 Entropy production and fluctuations

Fluctuations may be included in our formulation by using the ideas of Fluctuating Hydrodynamics [18,19]. We need to find the entropy production and write it as sum of generalized forces and fluxes. Then both the forces and the fluxes are identified. The linear relations between forces and fluxes then yield the correlations of the fluctuating quantities to be added to the equations of motion.

To find the production of entropy, we need to derive a few formulas. Multiplying the conservative equations of motion for the model (16) by  $u_i$  and summing, we obtain

$$\frac{d}{dt} \sum_{l,m,n} \sum_i \frac{a^2}{2} u_i^2 + W(l,m;n;t) = 0; \quad (26)$$

after some algebra. Provided viscous terms are included in the equation of motion, as in Eq. (24), we find

$$\frac{d}{dt} \sum_{l,m,n} \sum_i \frac{a^2}{2} u_i^2 + W(l,m;n;t) = \sum_{l,m,n} \sum_{i,j} u_i D_j [(i_j + i_j) g^0 (\partial_j^+ u_i)] : (27)$$

Let  $D_j = \frac{1}{a} \frac{\partial}{\partial x_j}$ , where  $\frac{1}{a} = (l,m;n)$  is a function of the point  $(l,m;n)$ . (Then  $\frac{1}{a} = (l-1,m;n)$  for  $j=1$ , and so on). We have  $D_j = D_j(\frac{1}{a})$ , and

$$\begin{aligned} \sum_{l,m,n} D_j &= \sum_{l,m,n} D_j \left( \frac{1}{a} \right) = \sum_{l,m,n} D_j \\ &= \sum_{l,m,n} D_j \left( \frac{1}{a} \right) = \sum_{l,m,n} D_j^+ ; \end{aligned} \quad (28)$$

after a trivial relabelling of indices. Using this formula, Eq. (27) becomes



$$\begin{aligned} \frac{d}{dt} \left( \frac{1}{2} \rho \mathbf{u}_i^2 + W(\mathbf{l}; \mathbf{m}; \mathbf{n}; \mathbf{t}) \right) &= \sum_{l,m,n,i,j} \mathbf{D}_j \cdot \mathbf{u}_i \cdot \mathbf{g}^0(\mathbf{D}_j^+ \mathbf{u}_i) \cdot \mathbf{e}_{ij}; \quad (29) \\ &= \sum_{l,m,n,i,j} \mathbf{g}^0(\mathbf{D}_j^+ \mathbf{u}_i) \cdot \mathbf{D}_j^+ \mathbf{u}_i = \sum_{l,m,n,i,j} \mathbf{e}_{ij}; \end{aligned}$$

where the symmetry of the viscous stress tensor has been used to derive the last equality. Eq. (29) describes the production of internal energy due to viscous processes.

If the temperature is not homogeneous, we need to replace the strain energy density to leading order by the elastic Helmholtz free energy density:

$$F(\mathbf{u}; T) = F_0(T) - (T - T_0) \mathbf{e}_{ij} \mathbf{e}_{ij} + \frac{1}{2} c_{ijkl} \mathbf{e}_{ij} \mathbf{e}_{kl}; \quad (30)$$

in which the symmetric tensor  $\mathbf{e}_{ij}$  describes anisotropic thermal expansion and sum over repeated indices is again implied [21]. Here the material is undeformed at temperature  $T_0$  in the absence of external forces and we assume that the temperature change  $(T - T_0)$  which accompanies thermoelastic deformation is small (linear thermoelasticity). The stress tensor is now

$$\mathbf{e}_{ij} = c_{ijkl} \mathbf{e}_{kl} - \mathbf{e}_{ij} (T - T_0); \quad (31)$$

which should be inserted in the equations of motion (16) or (24). The entropy density is  $S(\mathbf{u}; T) = -dF_0/dT + \mathbf{e}_{ij} \mathbf{e}_{ij}$  if we ignore the temperature dependence of the elastic constants. Heat conduction is governed by the equation  $T \partial S / \partial t = -\partial q_i / \partial x_i$ , i.e.,

$$c \frac{\partial T}{\partial t} + \mathbf{e}_{ij} T \frac{\partial \mathbf{e}_{ij}}{\partial t} = -\frac{\partial q_i}{\partial x_i}; \quad q_i = -\mathbf{e}_{ij} \frac{\partial T}{\partial x_j}; \quad (32)$$

Here  $c$  is the specific heat of the solid and  $\mathbf{e}_{ij}$  is the symmetric thermal conductivity tensor. These equations become

$$acT + a \mathbf{e}_{ij} T \mathbf{g}^0(\mathbf{D}_j^+ \mathbf{u}_i) \mathbf{D}_j^+ \mathbf{u}_i = -\mathbf{D}_i \cdot \mathbf{Q}_i; \quad \mathbf{Q}_i = -\mathbf{e}_{ij} \frac{\mathbf{D}_j^+ T}{a}; \quad (33)$$

after discretizing. Eq. (29) can be rewritten as

$$\begin{aligned} \frac{d}{dt} \left( \frac{1}{2} \rho \mathbf{u}_i^2 + W(\mathbf{l}; \mathbf{m}; \mathbf{n}; \mathbf{t}) \right) &= \sum_{l,m,n,i,j} \mathbf{D}_j \cdot \mathbf{u}_i \cdot \mathbf{g}^0(\mathbf{D}_j^+ \mathbf{u}_i) \cdot \frac{\mathbf{Q}_j}{a}; \quad (34) \\ &= \sum_{l,m,n,j} \mathbf{e}_{ij} \cdot \frac{\mathbf{D}_j \cdot \mathbf{Q}_j}{a}; \end{aligned}$$

The right side of this equation is related to the specific entropy (entropy per unit mass)  $s$  by

$$aT \frac{\partial s}{\partial t} = a \sum_{ij} \dot{e}_{ij} \sum_j D_j Q_j : \quad (35)$$

This can be written as

$$\frac{\partial s}{\partial t} = \sum_{ij} \dot{e}_{ij} \frac{1}{T} \sum_j D_j Q_j = \sum_{ij} \dot{e}_{ij} \frac{1}{T} + \sum_j Q_j D_j \frac{1}{aT} \sum_j D_j \frac{Q_j}{aT};$$

and summing over all points, we find the entropy production:

$$a^3 \sum_{lmn} \frac{1}{4} \frac{\partial (s)}{\partial t} + \sum_j D_j \frac{Q_j}{aT} = \sum_{lmn} \sum_{ij} a^3 \dot{e}_{ij} \frac{1}{T} + \sum_j Q_j D_j \frac{a^2}{T} : \quad (36)$$

This means that the generalized forces associated to the generalized velocities  $\dot{e}_{ij}$  and  $Q_j$  are  $a^3 \dot{e}_{ij} = T$  and  $a^2 D_j^+ (1/T)$ , respectively. Eqs.  $\dot{e}_{ij} = \dot{e}_{ijlm} \dot{e}_{lm}$  and  $Q_i = (T^2 = a) \dot{e}_{ij} D_j^+ (1/T)$  then imply that the kinetic coefficients associated to  $\dot{e}_{ij}$  and  $Q_j$  are  $k_B T \dot{e}_{ijlm} = a^3$  and  $k_B T^2 \dot{e}_{ij} = a^3$ , respectively. Following Onsager's ideas as used in Fluctuating Hydrodynamics [18,19,20], we conclude that the equations of motion including thermoelectric effects, dissipation and zero-mean fluctuations are as follows

$$a^2 \dot{u}_i = \sum_j D_j [(e_{ij} + \dot{e}_{ij} + s_{ij}) g^0(D_j^+ u_i)]; \quad (37)$$

$$h s_{ij} = 0;$$

$$h s_{ij}(l; m; n; t) s_{ab}(l^0; m^0; n^0; t^0) = k_B T \frac{\dot{e}_{ijab} + \dot{e}_{abij}}{a^3} \delta_{lm m^0} \delta_{nn^0} (t - t^0); \quad (38)$$

$$cT + T \sum_{ij} \dot{e}_{ij} g^0(D_j^+ u_i) D_j^+ u_i = \frac{1}{a} \sum_i D_i (Q_i + \dot{e}_i); \quad (39)$$

$$h \dot{e}_i = 0;$$

$$h \dot{e}_i(l; m; n; t) \dot{e}_j(l^0; m^0; n^0; t^0) = k_B T^2 \frac{\dot{e}_{ij} + \dot{e}_{ji}}{a^3} \delta_{lm m^0} \delta_{nn^0} (t - t^0); \quad (40)$$

with  $\dot{e}_{ij}$  given by (31). In principle, fluctuations can be included in boundary conditions by using the nonequilibrium fluctuating hydrodynamics formalism as explained in [23] and in [24] for the case of semiconductor interfaces. In crystals with cubic symmetry, the elastic constants and the viscosity tensor are given by Eqs. (4) and (22), respectively. The thermal conductivity and thermal expansion tensors are isotropic,  $\dot{e}_{ij} = \dot{e}_{ij}$ ,  $\dot{e}_{ij} = \dot{e}_{ij}$ . Note that the correlations of  $s_{ij}$  in (38) and of  $\dot{e}_i$  in (40) are proportional to  $1/a^3$ , which becomes  $(x - x^0)$  in the continuum limit as  $a \rightarrow 0$ .

Note that in our model, dissipation and fluctuations affect all atoms of the cubic lattice although we would expect from physical considerations that dissipation and fluctuations should be more pronounced near the core of moving dislocations, as they are directly related to the motion of the atomic constituents in the core vicinity. However our model should also fulfill these expectations. Why? Dissipation is described by a Rayleigh dissipative function that is a quadratic functional of the strain rate tensor, which, in turn, depends on the discrete distortion tensor. Since the distortion tensor (containing finite differences of the displacement vector) and its rate are larger near the core of defects, we expect that dissipation will be stronger near the core of a moving dislocation than at its far field. Fluctuations are introduced via the fluctuation-dissipation theorem and they should also be stronger near the core of moving dislocations.

#### 4 Models of fcc and bcc crystals with one atom per lattice site

In this Section, we explain how to extend our discrete models of dislocations to fcc or bcc crystal symmetry, assuming that we have one atom per lattice site [17]. For fcc or bcc crystals, the primitive vectors of the unit cell are not orthogonal. To find a discrete model for these crystals, we should start by writing the strain energy density in a non-orthogonal vector basis,  $a_1, a_2, a_3$ , instead of the usual orthonormal vector basis  $e_1, e_2, e_3$  determined by the cube sides. Let  $x_i$  denote coordinates in the basis  $e_i$ , and let  $x_i^0$  denote coordinates in the basis  $a_i$ . Notice that the  $x_i$  have dimensions of length while the  $x_i^0$  are dimensionless. The matrix  $T = (a_1; a_2; a_3)$  whose columns are the coordinates of the new basis vectors in terms of the old orthonormal basis can be used to change coordinates as follows:

$$x_i^0 = T_{ij}^{-1} x_j; \quad x_i = T_{ij} x_j^0 \quad (41)$$

Similarly, the displacement vectors in both basis are related by

$$u_i^0 = T_{ij}^{-1} u_j; \quad u_i = T_{ij} u_j^0 \quad (42)$$

and partial derivatives obey

$$\frac{\partial}{\partial x_i^0} = T_{ji} \frac{\partial}{\partial x_j}; \quad \frac{\partial}{\partial x_i} = T_{ji}^{-1} \frac{\partial}{\partial x_j^0} \quad (43)$$

Note that  $u_i^0$  and  $x_i^0$  are nondimensional while  $u_i$  and  $x_i$  have dimensions of length. By using these equations, the strain energy density  $W = (1/2) C_{iklm} e_{ik} e_{lm}$  can be written as

$$W = \frac{1}{2} c_{ijkl} \frac{\partial \alpha_i}{\partial x_j} \frac{\partial \alpha_l}{\partial x_m} = \frac{1}{2} c_{rspq}^0 \frac{\partial u_r^0}{\partial x_s^0} \frac{\partial u_p^0}{\partial x_q^0}; \quad (44)$$

where the new elastic constants are:

$$c_{rspq}^0 = c_{ijkl} T_{ir} T_{sj}^{-1} T_{lp} T_{qm}^{-1}; \quad (45)$$

Notice that the elastic constants have the same dimensions in both the orthogonal and the non-orthogonal basis. To obtain a discrete model, we shall consider that the dimensionless displacement vector  $u_i^0$  depends on dimensionless coordinates  $x_i^0$  that are integer numbers  $u_i^0 = u_i^0(l; m; n; t)$ . As in Section 2, we replace the distortion tensor (gradient of the displacement vector in the non-orthogonal basis) by a periodic function of the corresponding forward difference,  $w_i^{(j)} = g(D_j^+ u_i^0)$ . As in Eq. (11),  $g$  is a periodic function with  $g^0(0) = 1$  and period 1. The discretized strain energy density is

$$W(l; m; n; t) = \frac{1}{2} c_{rspq}^0 g(D_s^+ u_r^0) g(D_q^+ u_p^0); \quad (46)$$

The elastic constants  $c_{rspq}^0$  in (45) can be calculated in terms of the Voigt stiffness constants for a cubic crystal,  $C_{11}$ ,  $C_{44}$  and  $C_{12}$ , which determine the tensor of elastic constants (4). The elastic energy can be obtained from Eq. (46) for  $W$  by means of Eqs. (7). Then the conservative equations of motion (8) are

$$a^3 \frac{\partial^2 u_i^0}{\partial t^2} = T_{iq}^{-1} T_{pq}^{-1} \frac{\partial V}{\partial u_p^0};$$

which, together with Eqs. (7) and (46), yield

$$\frac{\partial^2 u_i^0}{\partial t^2} = T_{iq}^{-1} T_{pq}^{-1} D_j [g^0(D_j^+ u_p^0) c_{pjrs}^0 g(D_s^+ u_r^0)]; \quad (47)$$

This equation becomes (9) for orthogonal coordinates,  $T_{iq}^{-1} = \delta_{iq} = a$ .

To add dissipation and fluctuations to these equations, we need to replace  $c_{pjrs}^0 g(D_s^+ u_r^0)$  by  $c_{pjrs}^0 g(D_s^+ u_r^0) + \tau_{pj}^0 (T - T_0) + \tau_{pjrs}^0 g^0(D_s^+ u_r^0) D_s^+ u_r^0 + s_{pj}^0$ , in which  $\tau_{pjrs}^0$  is related to the viscosity tensor (22) in the same way as  $c_{pjrs}^0$  is related to  $c_{ijkl}$  by (45). The random stress tensor  $s_{pj}^0$  has zero mean and correlation given by (38) with the modified viscosity tensor  $\tau_{ijab}^0$  instead of the viscosity tensor (22). The heat conduction equations are

$$c \frac{\partial T}{\partial t} + T \tau_{ij}^0 g^0(D_j^+ u_i^0) D_j^+ \frac{\partial u_i^0}{\partial t} = D_i \tau_{ij}^0 D_j^+ T + \frac{\tau_i^0}{a}; \quad (48)$$

$$h_{ii}^0 = 0;$$

$$h_{ij}^0(l; m; n; t) - h_{ji}^0(l^0; m^0; n^0; t^0) = k_B T^2 \frac{h_{ij}^0 + h_{ji}^0}{a} \frac{1}{11^0 m m^0 n n^0} (t - t^0); \quad (49)$$

$$h_{pq}^0 = T_{pi}^{-1} T_{qj}^{-1} h_{ij}; \quad h_{pq}^0 = \frac{1}{2} (T_{ip} T_{qj}^{-1} + T_{jp} T_{qi}^{-1}) h_{ij}; \quad (50)$$

Note that the both the original and the modified tensors  $h_{ij}$  and  $h_{ij}^0$  are symmetric.

Once we have derived the equations of motion, stationary dislocations can be calculated by first finding the corresponding solution to the equations of anisotropic elasticity and using it to set up initial and boundary conditions for overdamped equations of motion. For fcc and bcc crystals, screw and edge dislocations have been constructed in Ref. [17].

## 5 Models for diamond and zincblende structures

Silicon and gallium arsenide are semiconductors of great importance for industry that crystalize in the face centered cubic (fcc) system. Crystals of these materials can be described as a fcc Bravais lattice with a basis of two atoms per site, which constitute a diamond structure for Si and a zincblende structure for GaAs [25]. When growing layers of these materials, defects are very important because they act as nucleation sites, and have to be eliminated after the growth process has ceased. Among defects, dislocations and misfit dislocations are often observed [5,4]. Thus, it is desirable to have an economic description of these defects and their dynamics in terms of control parameters such as temperature [12]. A molecular dynamics description is very costly if we need to couple atomic details in the nanoscale to a mesoscopic description in larger scales that are important in the growth process [26]. In this Section, we extend the previous models for cubic crystals with an atom per lattice site to crystals having two atoms per site (extension to crystals with more than two atoms per site is straightforward). Having two or more atoms per site introduces new features that are better explained revisiting the classic Born-von Karman work on vibrations of a linear diatomic chain [27]. We shall show how to obtain the wave equation for acoustic phonons in the elastic limit, directly from the equations for the diatomic chain. A similar calculation allows us in Subsection 5.2 to obtain the Cauchy equations for anisotropic elasticity in the continuum limit of our discrete models, which are constructed with the aim of having exactly this property. Subsection 5.3 shows how to calculate static dislocations for GaAs and Si.

## 5.1 Continuum limit for the linear diatomic chain

We shall consider a diatomic chain comprising alternatively atoms of masses  $M_1$  and  $M_2$  whose equilibrium positions are separated a distance  $a=2$ . The atoms are restricted to move only along the length of the chain. Their displacement with respect to their equilibrium positions will be denoted by a  $u_l$  and a  $v_l$ , respectively, in which  $l$  is the cell index, and  $u_l$  and  $v_l$  are dimensionless. If  $\Phi$  is the quadratic potential of interaction between neighboring atoms, the equations of motion for the diatomic chain are [27]

$$\begin{aligned} M_1 u_l &= \frac{1}{a} \left[ \Phi(v_l - u_l) + \frac{a}{2} \left[ \Phi(u_l - v_{l+1}) + \frac{a}{2} \right. \right. \\ &= \left. \left. \frac{a}{2} \right] [(v_l - u_l) - (u_l - v_{l+1})] \right]; \end{aligned} \quad (51)$$

$$\begin{aligned} M_2 v_l &= \frac{1}{a} \left[ \Phi(u_{l+1} - v_l) + \frac{a}{2} \left[ \Phi(v_l - u_l) + \frac{a}{2} \right. \right. \\ &= \left. \left. \frac{a}{2} \right] [(u_{l+1} - v_l) - (v_l - u_l)] \right]; \end{aligned} \quad (52)$$

If we assume that the solutions of these equations are plane waves,

$$u_l = U e^{i(2\pi l / \lambda)}; \quad v_l = V e^{i(2\pi l / \lambda)}; \quad (53)$$

the following dispersion relation is obtained

$$\omega^2 = \frac{\Phi(a=2)}{M_1 M_2} [(M_1 + M_2) \mp \sqrt{(M_1 + M_2)^2 - 4M_1 M_2 \sin^2 \frac{ka}{2}}]; \quad (54)$$

in which the minus (resp., plus) sign corresponds to the acoustic (resp., optic) branch of the dispersion relation [27]. Moreover, the corresponding amplitude ratio for the acoustic branch is

$$\frac{U}{V} = \frac{M_2 (1 + e^{i2\pi a / \lambda})}{(M_1 - M_2) \mp \sqrt{(M_1 + M_2)^2 - 4M_1 M_2 \sin^2 \frac{ka}{2}}}; \quad (55)$$

with a similar formula for the optical branch [27]. In the long wavelength limit,  $\lambda \rightarrow \infty$ , the acoustic vibrations satisfy

$$U = V; \quad \omega = c \frac{2\pi}{a}; \quad (56)$$

$$c = \frac{v}{c} \frac{\Phi(a=2) a^2}{2(M_1 + M_2)} = \sqrt{\frac{E}{\rho}}; \quad (57)$$

$$= \frac{M_1 + M_2}{a}; \quad E = \frac{\rho(a=2)a}{2}; \quad (58)$$

In these equations,  $E$  and  $\rho$  are the Young modulus and the linear mass density, respectively [27]. In the limit as  $a \rightarrow 0$ , each cell comprising two atoms moves rigidly with a phase velocity  $c$  and a wave number  $2\pi/a$ .

The continuum limit of the diatomic chain equations recovers the acoustic vibrations only. In this limit,  $l \rightarrow 1$  and  $a \rightarrow 0$ , with fixed  $x = la$ . Furthermore,

$$au_1(t) = u(la, t) = u(x, t); \quad av_1(t) = u\left(la + \frac{a}{2}, t\right) = u\left(x + \frac{a}{2}, t\right); \quad (59)$$

If we now add Eqs. (51) and (52) divide by  $a$ , and use (59) to approximate the result, we obtain the following wave equation in the continuum limit:

$$\frac{\partial^2 u}{\partial t^2} = E \frac{\partial^2 u}{\partial x^2}; \quad (60)$$

provided  $\rho$  and  $E$  are given by Eq. (58). The wave speed  $c$  is then given by Eq. (57). Equation (60) is the elastic continuum limit of the diatomic chain equations, which does not contain optical vibrations.

## 5.2 Discrete model for a fcc lattice with a two-atom basis

We shall now propose a discrete model for a fcc lattice with a basis comprising two atoms, of masses  $M_1$  and  $M_2$ , respectively. Although this model is much more complicated to describe, the key ideas to show that it is compatible with anisotropic elasticity are the same as in Subsection 5.1 for the diatomic chain.

The main ideas needed to write a model for this crystal structure are the following:

- (1) Write the strain energy corresponding to a fcc crystal in a non-orthogonal basis with axes given by the usual primitive directions of the fcc Bravais lattice.
- (2) Write the corresponding strain energy for a fcc crystal with two atoms per lattice site.
- (3) Restore the periodicity of the crystal by defining the discrete distortion tensor as a periodic function (with period 1) of the discrete gradient of the displacement vector.
- (4) Define the potential energy of the crystal as the strain energy times the volume of the unit cell summed over all lattice sites. Then write down the equations of motion for the displacement vectors at each site.

- (5) Check that the continuum limit of the model yields the usual anisotropic elasticity.

We shall now carry out this program, which is an extension of that presented in Section 4 for a fcc lattice with a single atom per site; see also Ref. [17]. The primitive vectors of the fcc lattice are

$$a_1 = \frac{a}{2} (0;1;1); \quad a_2 = \frac{a}{2} (1;0;1); \quad a_3 = \frac{a}{2} (1;1;0); \quad (61)$$

in terms of the usual orthonormal vector basis  $e_1, e_2, e_3$  determined by the cube. From these vectors, we determine the matrix  $T_{ij}$  to change coordinates as in (41) and (42). In the continuum limit, the strain energy is given by (44) with elastic constants given by (45) and (4).

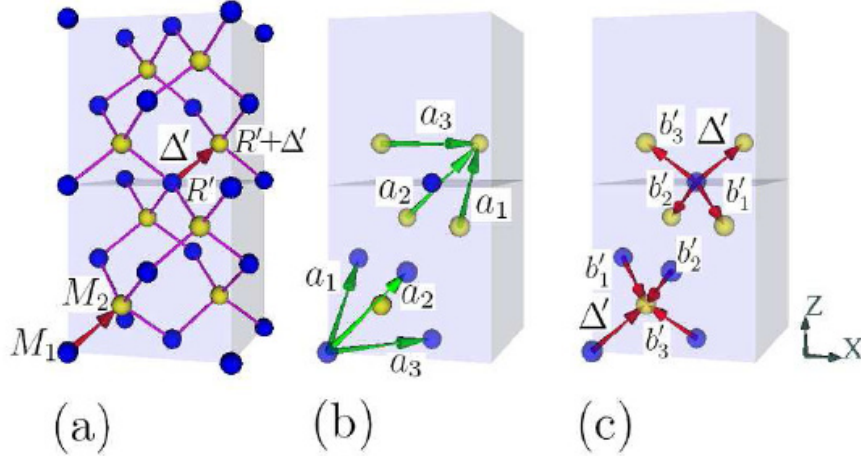


Fig. 1. Relevant vectors joining lattice points that are needed to discretize the displacement field in a zincblende lattice. All coordinates are expressed in the non-orthogonal basis spanned by the primitive vectors  $a_1, a_2$ , and  $a_3$ . (a) The basis of a unit cell placed at  $R^0 = (l; m; n)$  comprises one atom of mass  $M_1$  with displacement vector  $u_i^0(R^0; t)$  and one atom of mass  $M_2$  and displacement vector  $v_i^0(R^0 + a_i; t)$ . (b) Discrete gradients involving lattice points closest to  $R^0$  (resp.  $R^0 + a_i$ ) are backward differences from  $R^0 + a_i$  (resp., forward differences from  $R^0$ ) along the primitive directions:  $D_j^- v_i^0(R^0 + a_i; t)$ , (resp.,  $D_j^+ u_i^0(R^0; t)$ ),  $i, j = 1; 2; 3$ . (c) The auxiliary vectors  $b'_i$  satisfy  $a_i^0 + b'_i = 0$ ,  $i = 1; 2; 3$ .

Once we have written the strain energy of a fcc crystal in the non-orthogonal basis spanned by the primitive vectors, we can introduce our discrete model. We shall consider a fcc lattice with a two-atom basis. In equilibrium, atoms with mass  $M_1$  will be placed at the lattice sites, so that their displacement vectors will depend on integer numbers and time:  $u_i^0 = u_i^0(l; m; n; t)$ . In equilibrium, atoms with mass  $M_2$  will be placed at the sites of a fcc lattice which, in the orthonormal basis  $e_i$ , is rigidly displaced by a vector  $\mathbf{r} = (a/4; a/4; a/4)$  with respect to the first fcc lattice; see Fig. 1. In terms of the non-orthogonal basis  $a_i$ , the vector  $(a/4; a/4; a/4)$  becomes  $\mathbf{r}^0 = (1/4; 1/4; 1/4)$ .



We should define discrete differences of a displacement vector so that a discrete difference become the corresponding partial derivative in the continuum limit. This requirement can be satisfied in more than one way using different neighbors of a given lattice point. We shall select only two neighbors of a lattice point for this purpose, using that the nearest neighbors of an atom with mass  $M_1$  are atoms with mass  $M_2$  and viceversa. Fig. 1 shows that each atom with mass  $M_1$  (resp.,  $M_2$ ) is linked to its four nearest neighbors having mass  $M_2$  (resp.,  $M_1$ ) by  $\vec{a}_i^0$ ,  $\vec{b}_i^0 = -\vec{a}_i^0$  (resp.,  $\vec{a}_i^0$ ;  $\vec{b}_i^0$ ). Thus the nearest neighbors of an atom with displacement vector  $\vec{v}_i^0(\vec{R}^0 + \vec{a}_j^0; t)$  have displacement vectors  $\vec{u}_i^0(\vec{R}^0; t)$  and  $\vec{u}_i^0(\vec{R}^0 + \vec{a}_j^0; t)$ , with  $j = 1; 2; 3$ , and the nearest neighbors of an atom with displacement vector  $\vec{u}_i^0(\vec{R}^0; t)$  have displacement vectors  $\vec{v}_i^0(\vec{R}^0 + \vec{a}_j^0; t)$  and  $\vec{v}_i^0(\vec{R}^0 + \vec{b}_j^0; t)$ , with  $j = 1; 2; 3$ . These facts motivate our definition of discrete differences of a displacement vector.

Let us define the standard forward and backward difference operators along the primitive directions as

$$D_j f(\vec{R}^0) = [f(\vec{R}^0 + \vec{a}_j^0) - f(\vec{R}^0)]: \quad (62)$$

Then  $\nabla_{ij}^{(2)}(\vec{R}^0 + \vec{a}_j^0; t) = D_j^+ \vec{u}_i^0(\vec{R}^0; t)$  is the discrete gradient of the displacement vector  $\vec{v}_i^0(\vec{R}^0 + \vec{a}_j^0; t)$  which involves lattice points closest to  $\vec{R}^0 + \vec{a}_j^0$ , whereas  $\nabla_{ij}^{(1)}(\vec{R}^0; t) = D_j^- \vec{v}_i^0(\vec{R}^0 + \vec{a}_j^0; t)$  is the discrete gradient of the displacement vector  $\vec{u}_i^0(\vec{R}^0; t)$  which involves lattice points closest to  $\vec{R}^0$ . The distortion tensor of our discrete model at the cell  $\vec{R}^0$  could be defined as a weighted average of  $g(\nabla_{ij}^{(1)})$  and  $g(\nabla_{ij}^{(2)})$ , in which  $g(\mathbf{x})$  is a period-one periodic function such that  $g(\mathbf{x}) = \mathbf{x}$  as  $\mathbf{x} \rightarrow 0$ . For simplicity, we shall adopt equal weights in our definition:

$$w_i^{(j)}(\vec{R}^0; t) = \frac{g(\nabla_{ij}^{(2)}) \vec{u}_i^0(\vec{R}^0; t) + g(\nabla_{ij}^{(1)}) \vec{v}_i^0(\vec{R}^0 + \vec{a}_j^0; t)}{2}: \quad (63)$$

Obviously, this is reasonable for materials such as Si having a diamond structure, and also in the case of atoms of similar size for materials with zincblende structure. In the continuum limit  $a \rightarrow 0$ , the distortion tensor tends to the gradient of the displacement vector:

$$w_i^{(j)} = \frac{\partial \alpha_i^0}{\partial x_j^0}: \quad (64)$$

In practice, the period-one function  $g$  should be fitted to experimental or molecular dynamics data, such as the Peierls stress needed for a dislocation to move; see Fig. 1 of Ref. [17] for the variation of the Peierls stress as a function of the parameter controlling the shape of a piecewise linear function  $g$ . The positive potential energy of the crystal will therefore be

$$V = \frac{a^3}{4} \sum_{lm, n} \frac{1}{8} c_{rspq}^0 [g(\mathbb{D}_s^+ u_r^0) + g(\mathbb{D}_s^- v_r^0)] [g(\mathbb{D}_q^+ u_p^0) + g(\mathbb{D}_q^- v_p^0)] : \quad (65)$$

Here  $a^3=4$  is the volume spanned by the three primitive vectors.

The conservative equations of motion are

$$M_1 \frac{\partial^2 u_i^0}{\partial t^2} = T_{iq}^{-1} T_{pq}^{-1} \frac{\partial V}{\partial u_p^0} : \quad (66)$$

$$M_2 \frac{\partial^2 v_i^0}{\partial t^2} = T_{iq}^{-1} T_{pq}^{-1} \frac{\partial V}{\partial v_p^0} : \quad (67)$$

Using Eq. (65), these equations become

$$\frac{4M_1}{a^3} \frac{\partial^2 u_i^0}{\partial t^2} = \frac{1}{4} T_{iq}^{-1} T_{pq}^{-1} D_j f c_{pjrs}^0 g^0(\mathbb{D}_j^+ u_p^0) [g(\mathbb{D}_s^- v_r^0) + g(\mathbb{D}_s^+ u_r^0)] g; \quad (68)$$

$$\frac{4M_2}{a^3} \frac{\partial^2 v_i^0}{\partial t^2} = \frac{1}{4} T_{iq}^{-1} T_{pq}^{-1} D_j f c_{pjrs}^0 g^0(\mathbb{D}_j^- v_p^0) [g(\mathbb{D}_s^+ u_r^0) + g(\mathbb{D}_s^- v_r^0)] g; \quad (69)$$

If  $M_1 = M_2$  (the case of Si), this system of equations is invariant under the symmetry:  $u_i^0(R^0) \leftrightarrow v_i^0(R^0 + \frac{1}{2})$ . To obtain the continuum limit, we add Eqs. (68) and (69), take into account the continuum limit (64), and use Eqs. (41) to revert to the dimensional orthogonal coordinates. Then the resulting equations are those of anisotropic elasticity:

$$\frac{\partial^2 \alpha_i}{\partial t^2} = \frac{\partial}{\partial x_j} C_{ijrs} \frac{\partial \alpha_r}{\partial x_s} : \quad (70)$$

In this equation, the mass density is the sum of the masses in the primitive cell divided by the volume thereof:

$$= \frac{M_1 + M_2}{a^3=4} : \quad (71)$$

Fluctuations and dissipation can be added to these equations in the same way as for the models with one-atom basis. The derivation of these equations in non-orthogonal coordinates follows those in Sections 2 and 3, but using the following energy instead of (27):

$$\frac{d}{dt} \sum_{lm, n} \frac{1}{4} \sum_i \frac{1}{2} \sum_j T_{ij} u_j^{0A} + \sum_{rspq} \frac{1}{2} c_{rspq}^0 g(\mathbb{D}_s^+ u_r^0) g(\mathbb{D}_q^+ u_p^0)$$

$$= \sum_{lm} \sum_{ijn} \mathbf{u}_i^0 \mathbf{D}_j [ \mathbf{g}_{ij}^0 \mathbf{D}_j^+ \mathbf{u}_i^0 ] : \quad (72)$$

In particular, (36) also holds in non-orthogonal coordinates, which then yields the same formulas for the fluctuations as in orthogonal coordinates. For a zincblende structure, the governing equations including dissipation and fluctuations are:

$$\begin{aligned} c \frac{\partial T}{\partial t} + \frac{T}{2} \mathbf{g}_{ij}^0 \mathbf{g}^0 \mathbf{D}_j^+ \mathbf{u}_i^0 \mathbf{D}_j^+ \frac{\partial \mathbf{u}_i^0}{\partial t} + \mathbf{g}^0 \mathbf{D}_j \mathbf{v}_i^0 \mathbf{D}_j \frac{\partial \mathbf{v}_i^0}{\partial t} \\ = \mathbf{D}_i \mathbf{g}_{ij}^0 \mathbf{D}_j^+ T + \frac{\dot{\mathbf{u}}_i^0}{a} ; \end{aligned} \quad (73)$$

$$h_{ij}^0 = 0;$$

$$h_{ij}^0(l;m;n;t) \mathbf{g}_{ij}^0(l^0;m^0;n^0;t^0) = k_B T^2 \frac{\mathbf{g}_{ij}^0 + \mathbf{g}_{ji}^0}{a} \mathbb{1}^0_{mm^0 nn^0}(t-t^0); \quad (74)$$

$$\frac{4M_1}{a^3} \frac{\partial^2 \mathbf{u}_i^0}{\partial t^2} = \frac{1}{2} T_{iq}^{-1} T_{pq}^{-1} \mathbf{D}_j^+ f [ \mathbf{g}_{pj}^0 + \mathbf{g}_{pj}^0 + \mathbf{s}_{pj}^0 ] \mathbf{g}^0 \mathbf{D}_j^+ \mathbf{u}_p^0 g; \quad (75)$$

$$\frac{4M_2}{a^3} \frac{\partial^2 \mathbf{v}_i^0}{\partial t^2} = \frac{1}{2} T_{iq}^{-1} T_{pq}^{-1} \mathbf{D}_j^+ f [ \mathbf{g}_{pj}^0 + \mathbf{g}_{pj}^0 + \mathbf{s}_{pj}^0 ] \mathbf{g}^0 \mathbf{D}_j \mathbf{v}_p^0 g; \quad (76)$$

$$h_{ij}^0 = 0;$$

$$h_{ij}^0(l;m;n;t) s_{ab}^0(l^0;m^0;n^0;t^0) = k_B T \frac{\mathbf{g}_{ijab}^0 + \mathbf{g}_{abij}^0}{a^3} \mathbb{1}^0_{mm^0 nn^0}(t-t^0); \quad (77)$$

$$\mathbf{g}_{pj}^0 = c_{pjab}^0 \mathbf{e}_{ab}^0 \quad \mathbf{g}_{pj}^0 (T - T_0); \quad \mathbf{g}_{pj}^0 = \mathbf{g}_{pjab}^0 \mathbf{e}_{ab}^0; \quad (78)$$

together with (50). In these equations,  $\mathbf{e}_{ab}^0 = (\mathbf{w}_a^{(b)} + \mathbf{w}_b^{(a)})/2$  is the symmetric part of the distortion tensor (63).

### 5.3 Dislocations in Si and GaAs

Si and GaAs crystals are face-centred cubic with two atoms per lattice site, one at (0;0;0) and the other one at  $\mathbf{r} = (1/4;1/4;1/4)$ . Both atoms are identical in Si (diamond structure), whereas they are different in GaAs: one atom is gallium and the other arsenic (zincblende structure). Each atom is tetrahedrally bonded to four nearest-neighbors, and the shortest lattice vector  $\mathbf{h}_{110}/2$  links a second neighbor pair, as shown in Figure 2. The covalent bond between two atoms is strongly localized and directional, and this feature strongly affects the characteristics of dislocations. In turn, dislocations influence both mechanical and electrical properties of these semiconductors [4,10]. In this Section, we shall construct straight dislocations for Si and GaAs using their elastic stiffnesses and a method for calculating their strain field.

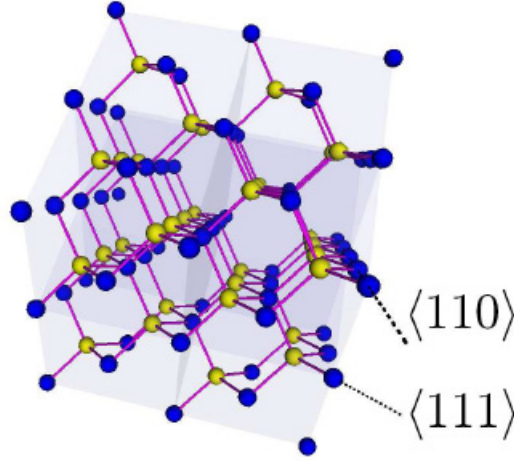


Fig. 2. Relevant directions in a fcc lattice with a two-atom basis.

Perfect dislocations have Burgers vectors  $b = \frac{1}{2} \langle 110 \rangle$  (the same as in the case of fcc lattices with a one-atom basis) and slip on the close packed  $\{111\}$  planes having normal vector  $n$ . Their dislocation line vectors usually lie along  $\langle 110 \rangle$  directions, forming  $60^\circ$  (perfect  $60^\circ$  dislocations) or  $0^\circ$  (perfect screw dislocations) with respect to the Burgers vector.

We will now construct a perfect screw and a perfect  $60^\circ$  dislocation for GaAs lattice, both having Burgers vector  $b = \frac{1}{2} \langle 110 \rangle$ . Gliding dislocations having this Burgers vector will leave behind a perfect crystal, since it is a primitive vector of the lattice [4]. For Si the same construction can be used.

The tensor of elastic constants is given by (4) in terms of the Voigt elastic stiffnesses  $C_{ij}$  and the degree of anisotropy  $H$  of (5). We use the following values of the Voigt stiffnesses measured in units of  $10^9$  Pa at room temperature ( $T = 298$  K) [28]:

$$C_{11} = 165.6; C_{12} = 63.98; C_{44} = 79.51; \quad \text{for Si}; \quad (79)$$

$$C_{11} = 118.8; C_{12} = 53.8; C_{44} = 58.9; \quad \text{for GaAs}. \quad (80)$$

Between 200 K and 800 K, these constants decrease linearly with increasing temperature, so that  $\frac{1}{C_{ij}} \frac{dC_{ij}}{dT} = -10^{-4} \text{ K}^{-1}$ ,  $i, j = 1, 2, 3$ , [29,30,31]. Such small corrections could be straightforwardly included in our calculations, modifying minimally our results.

To calculate the elastic far field of any stationary straight dislocation, we shall follow the method explained in Chapter 13 of Hirth and Lothe's book [10]. Firstly, we determine an orthonormal coordinate system  $e_1^0, e_2^0, e_3^0$  with  $e_3^0 = \frac{b}{|b|}$  parallel to the dislocation line and  $e_2^0 = n$  being the unitary vector normal to the glide plane. In terms of the new basis, the elastic displacement field  $(u_1^0; u_2^0; u_3^0)$  depends only on  $x_1^0$  and on  $x_2^0$ .

Secondly, we calculate the elastic constants in the reference system  $e_1^0, e_2^0, e_3^0$ :

$$c_{ijkl}^0 = c_{ijkl} - \sum_{n=1}^3 (S_{in} S_{jn} S_{kn} S_{ln} - \delta_{in} \delta_{jn} \delta_{kn} \delta_{ln}) \quad (81)$$

Here the rows of the orthogonal matrix  $S = (e_1^0; e_2^0; e_3^0)^t$  are the coordinates of the  $e_i^0$ 's in the old orthonormal basis  $e_1, e_2, e_3$ . In the new reference system, the Burgers vector has coordinates  $(b_1^0; b_2^0; b_3^0)$ .

Thirdly, the displacement vector  $(u_1^0; u_2^0; u_3^0)$  is calculated as follows:

Select three roots  $p; p_2; p_3$  with positive imaginary part out of each pair of complex conjugate roots of the polynomial  $\det[a_{ik}(p)] = 0$ ,  $a_{ik}(p) = c_{i1k1}^0 + (c_{i1k2}^0 + c_{i2k1}^0)p + c_{i2k2}^0 p^2$ .

For each  $n = 1; 2; 3$  find an eigenvector  $A_k(n)$  associated to the zero eigenvalue for the matrix  $a_{ik}(p_n)$ .

Solve  $\text{Re} \sum_{n=1}^3 A_i(n) D(n) = b_i^0$ , and  $\text{Re} \sum_{n=1}^3 \sum_{k=1}^3 (c_{i2k1}^0 + c_{i2k2}^0 p_n) A_k(n) D(n) = 0$ , in which  $i = 1; 2; 3$ , for the imaginary and real parts of  $D(1), D(2), D(3)$ .

For  $k = 1; 2; 3$ ,  $u_k^0 = \text{Re} \left[ \frac{1}{2} \sum_{n=1}^3 A_k(n) D(n) \ln(x_1^0 + p_n x_2^0) \right]$ .

Lastly, we can calculate the displacement vector  $u_k^0$  in the non-orthogonal basis  $a_i$  from  $u_k^0$ .

For the perfect 60° dislocation, we have

$$e_1^0 = \frac{1}{\sqrt{6}}(1; 1; 2); \quad e_2^0 = \frac{1}{\sqrt{3}}(-1; -1; 1); \quad e_3^0 = \frac{1}{\sqrt{2}}(-1; 1; 0); \quad (82)$$

and the resulting dislocation is depicted in Fig. 3.

For the pure screw dislocation, we have

$$e_1^0 = \frac{1}{\sqrt{6}}(-1; -2; 1); \quad e_2^0 = \frac{1}{\sqrt{3}}(-1; 1; 1); \quad e_3^0 = \frac{1}{\sqrt{2}}(-1; 0; 1); \quad (83)$$

and the resulting dislocation can be observed in Fig. 4.

## 6 Conclusions

We have proposed discrete models describing defects in crystal structures whose continuum limit is the standard linear anisotropic elasticity. The main

ingredients entering the models are the elastic stiffness constants of the material and a dimensionless periodic function that restores the translation invariance of the crystal (and together with the elastic constants determines the dislocation size). For simple cubic crystals, their equations of motion with conservative or damped dynamics (including fluctuations according as in Fluctuating Hydrodynamics) are derived. For fcc and bcc metals, the primitive vectors along which the crystal is translationally invariant are not orthogonal. Similar discrete models and equations of motion are found by writing the strain energy density and the equations of motion in non-orthogonal coordinates. In these latter cases, we can determine numerically stationary perfect edge and screw dislocations. We have also extended our discrete models to the case of fcc lattices with a two-atom basis, which includes important applications such as Si and GaAs crystals. For GaAs, we have calculated numerically two perfect dislocations which may be used to calculate the structure and motion of similar dislocations under stress as explained in Ref. [17]. Similarly to the case of the linear diatomic chain in which there are acoustic and optical branches of the dispersion relation, we expect that the dynamics of the discrete models with two-atom bases are richer than their continuum limits.

#### Acknowledgements

This work has been supported by the Spanish Ministry of Education grants MAT2005-05730-C02-01 (LLB and IP) and MAT2005-05730-C02-02 (AC), and by the Universidad Complutense grants Santander/UCM PR27/05-13939 and CM/UCM 910143 (AC). I. P. Lans was financed by the Spanish Ministry of Education. He acknowledges Prof. Russel Caisch and his Materials Modeling in Applied Mathematics group for their hospitality and fruitful discussions during a visit to UCLA and also Hyung-Jun Kim for his helpful explanations about the geometry of dislocations in Si.

#### References

- [1] Kim, H. J., Zhao, Z. M., Xie, Y. H., 2003. Three-stage nucleation and growth of Ge self-assembled quantum dots grown on partially relaxed SiGe buffer layers. *Phys. Rev. B* 68, 205312 (7 pages).
- [2] Zhao, Z. M., Hulko, O., Kim, H. J., Liu, J., Sugahara, T., Shi, B., Xie, Y. H., 2004. Growth and characterization of InAs quantum dots on Si(001) surfaces. *J. Crystal Growth* 271, 450-455.
- [3] Grahm, H. T. (editor), 1995. *Semiconductor Superlattices: Growth and Electronic Properties*. World Scientific, Singapore.

- [4] Hull, D., Bacon, D.J. 2001. Introduction to Dislocations, 4th edition. Butterworth-Heinemann, Oxford UK.
- [5] Matthews, J.W., Blakeslee, A.E., 1974. Defects in epitaxial multilayers. I. Misfit dislocations. J. Crystal Growth 27, 118-125.
- [6] Brune, H., Roder, H., Boragno, C., Kern, K., 1994. Strain relief at hexagonal-close-packed interfaces. Phys. Rev. B 49, 2997-3000.
- [7] Carter, C.B., Hwang, R.Q., 1995. Dislocations and the reconstruction of (111) fcc metal surfaces. Phys. Rev. B 51, 4730-4733.
- [8] Chen, J.-S., Mehraeen, S., 2004. Variationally consistent multi-scale modeling and homogenization of stressed grain growth. Comput. Meth. Appl. Mech. Engrg. 193, 1825-1848.
- [9] Nabarro, F.R.N., 1967. Theory of Crystal Dislocations. Oxford University Press, Oxford, UK.
- [10] Hirth, J.P., Lothe, J., 1982. Theory of Dislocations, 2nd edition. John Wiley and Sons, New York.
- [11] Freund, L.B., 1990. Dynamic Fracture Mechanics. Cambridge University Press, Cambridge UK.
- [12] Szuranyi, P., Clerly, D., eds., 1998. Special Issue on Control and use of defects in materials. Science 281, 939.
- [13] Holt, D.L., 1970. Dislocation cell formation in metals. J. Appl. Phys. 41, 3179-3201.
- [14] Rickman, J.M., Vinals, J., 1997. Modeling of dislocation structures in materials. Phil. Mag. A 75, 1251-1262.
- [15] Groma, I., Csikor, F.F., Zaiser, M., 2003. Spatial correlations and higher-order gradient terms in a continuum description of dislocation dynamics. Acta Mater. 51, 1271-1281.
- [16] Hahner, P., Bay, K., Zaiser, M., 1998. Fractal Dislocation Patterning During Plastic Deformation. Phys. Rev. Lett. 81, 24702473.
- [17] Carpio, A., Bonilla, L.L., 2005. Discrete models of dislocations and their motion in cubic crystals. Phys. Rev. B 71, 134105 (10 pages).
- [18] Landau, L.D., Lifshitz, E.M., 1959. Fluid Mechanics, Pergamon Press, London.
- [19] van Saarloos, W., Bedeaux, D., Mazur, P., 1982. Non-linear hydrodynamic fluctuations around equilibrium. Physica A 110, 147-170.
- [20] Romero-Rochón, V., Rubí, J.M., 1998. Discretized integral hydrodynamics. Phys. Rev. E 58, 18431850.
- [21] Landau, L.D., Lifshitz, E.M., 1986. Theory of elasticity, 3rd edition. Pergamon Press, London.

- [22] Carpio, A., Bonilla, L.L., 2003. Edge dislocations in crystal structures considered as traveling waves of discrete models. *Phys. Rev. Lett.* 90, 135502 (4 pages).
- [23] Bedeaux, D., Albano, A.M., Mazur, P., 1975. Boundary conditions and nonequilibrium thermodynamics. *Physica A* 82, 438-462.
- [24] Gomila, G., Rubi, J.M., 1998. Fluctuations generated at semiconductor interfaces. *Physica A* 258, 17-31.
- [25] Grahm, H. T., 1999. *Introduction to Semiconductor Physics*. World Sci., Singapore.
- [26] Gurev, M.F., Ratsch, C., Merriman, B., Caish, R.E., Osher, S., Zink, J.J., Vvedensky, D.D., 1998. Level-set methods for the simulation of epitaxial phenomena. *Phys. Rev. E* 58, R6927-R6930.
- [27] Born, M., Huang, K., 1954. *Dynamic Theory of Crystal Lattices*. Oxford University Press, Oxford, UK.
- [28] Hjort, K., Soderkvist, J., Schweitz, J.A., 1994. Gallium arsenide as a mechanical material. *J. Micromech. Microeng.* 4 (1994) 1-13.
- [29] Cottam, R.I., Saunders, G.A., 1973. Elastic constants of GaAs from 2 K to 320 K. *J. Phys. C: Solid State Phys.*, Vol 6 (13): 2105-2118.
- [30] Nikanorov, S.P., Burenkov, Yu.A., Stepanov, A.V., 1971. Elastic properties of silicon. *Sov. Phys. Solid State* 13 (10), 2516-2518, 1972 [*Fiz. Tverd. Tela* 13, 3001-3004].
- [31] Burenkov, Yu.A., Burdukov, Yu.M., Davidov, S.Yu., Nikanorov, S.P., 1973. Temperature dependences of the elastic constants of gallium arsenide. *Sov. Phys. Solid State* 15 (6), 1175-1177. [*Fiz. Tverd. Tela* 13, 1757-1761].



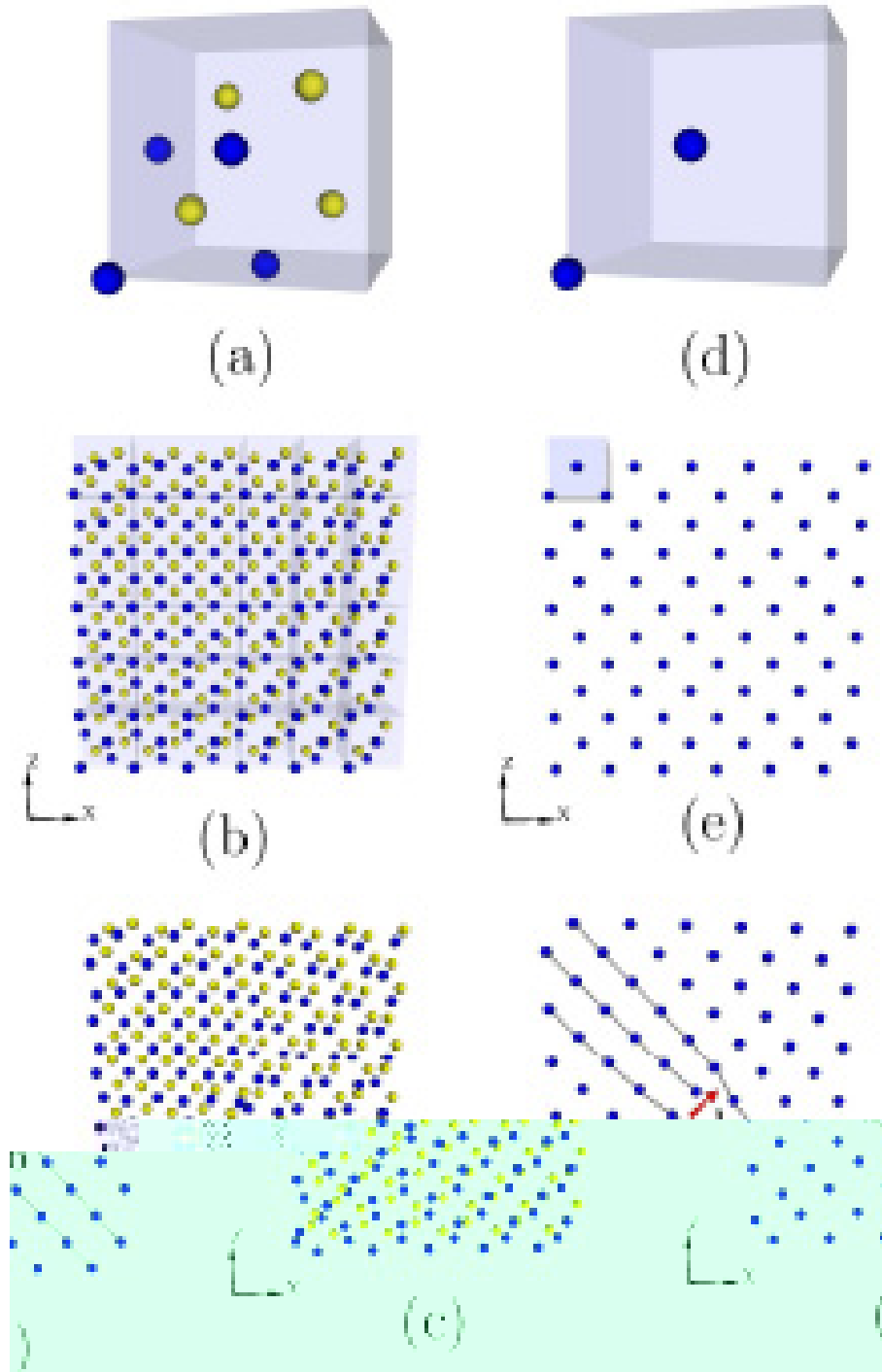


Fig. 3. Displacement field in a GaAs lattice created by a perfect 60° dislocation of Burgers vector  $\mathbf{b} = (1; 0; 1)/2$ . (a) Reference cubic cell with its eight atoms. (b) One layer of a perfect undistorted lattice. (c) The same layer distorted by a perfect 60° dislocation. Panels (d), (e) and (f) correspond to (a), (b) and (c), respectively but we have depicted only two atoms per reference cubic cell.

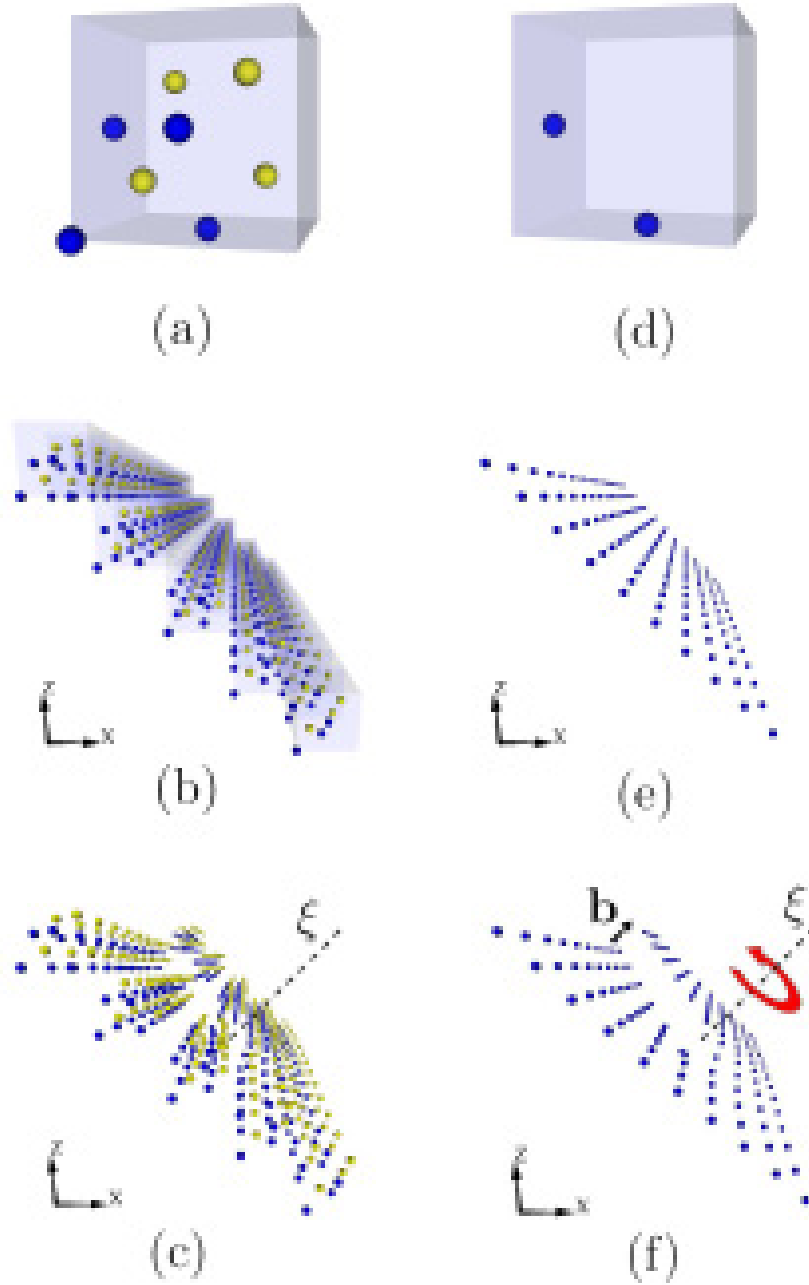


Fig. 4. Displacement field in a GaAs lattice created by a perfect screw dislocation of Burgers vector  $\mathbf{b} = (1;0;1)a/2$ . (a) Reference cubic cell with its eight atoms. (b) One layer of cubic cells normal to the Burgers vector for a perfect undistorted lattice. (c) The same layer distorted by a perfect screw dislocation. Panels (d), (e) and (f) correspond to (a), (b) and (c), respectively but we have depicted only two atoms per reference cubic cell.